Review chapter from **Solar System Ices**, *477-507*
Revised, 1995. B. Schmitt et al. (eds.) Kluwer Academic, 1998.

MARS CO_2 ICE POLAR CAPS

FRANÇOIS FORGET
Laboratoire de Météorologie Dynamique du CNRS
Ecole Normale Supérieure, 24 rue Lhomond,
75231 Paris Cedex 05, France.

1. Introduction

The Martian Polar caps have been observed for more than two centuries by terrestrial observers. Following the first observations by J. Cassini and C. Huygens, Herschel (1784) first described their seasonal characteristics. From Earth, they appear like white bright features waxing and waning over a Mars year. Because of the 25.1^o inclination of Mars'equator to its orbit plane, the seasons on Mars are much like their terrestrial counterparts.

By analogy with the Earth, most observers assumed that the Martian polar caps were composed of water frost, until the first space probes to Mars. Following the Mariner 4 mission in 1965, Leighton and Murray (1966) used a simple thermal model to reveal the processes which control the Martian seasonal polar caps: during the fall and winter seasons at high latitudes, the local surface and atmospheric temperatures become cold enough to reach the frost point of CO_2, the major constituent of the thin Martian atmosphere. CO_2 condenses and forms CO_2 ice deposits on the surface. During the spring and summer seasons in a given hemisphere, the seasonal CO_2 cap sublimates back into the atmosphere. Spectroscopic observations later confirmed the CO_2 composition (Herr and Pimentel, 1969; Larson and Fink, 1972).

This "CO_2 cycle" causes the global atmospheric mass to vary by several tens of percent. Surface pressure measurement made from the two Viking probes which landed in the northern hemisphere of the planet in 1976 clearly showed these enormous seasonal variations (fig. 1). Although these seasonal oscillations are also influenced by the atmospheric circulation (Hourdin *et al.*, 1993), they reflect the variation of the global mass of the atmosphere; the first minimum of pressure near sol 100 occurs during southern winter when a large part of the atmosphere is trapped in the seasonal south polar cap and the secondary minimum corresponds to the northern winter, shorter than the southern winter because of the high eccentricity of the Martian orbit. The CO_2 cycle also affects the Martian climate by creating a strong planetwide atmospheric circulation called the "condensation flow" which transports heat, momentum and mass from the subliming cap toward the region of the forming polar cap. It is also coupled in several ways (described in this chapter) to the seasonal cycles of H_2O and dust.

As can be seen, the influence of the Martian seasonal caps is not restricted to the high Martian latitudes, and understanding the processes that control the CO_2 cycle is important for understanding the past and current Martian climate.

The process of condensation and sublimation of the polar caps described by Leighton and Murray (1966) is rather simple, but the observations of the polar caps by the spacecraft missions of the 70's (Mariner 9 and Viking) gave unexpected results and even raised some of the most puzzling questions about the planet.

Our goal in this chapter is to summarize what we know about the Martian polar caps and their physics. Since the condensation and the sublimation phases differ in the processes involved and in the kind of observations available, we have chosen to first examine the formation of the polar caps (section 2) and then their sublimation phase (section 3). In the much shorter section 4, we briefly discuss the implications and the problems raised by the possibility that there is permanent CO_2 ice in the Martian polar regions.

2. Condensation of the Martian polar caps

2.1. OBSERVATIONS IN THE THERMAL INFRARED

Things start in fall, when the polar regions are shrouded in continual darkness during the polar night. Almost all that is known about the condensing polar caps has therefore come from the infrared observations by the two orbiting spacecraft missions to Mars: Mariner 9 and Viking.

These observations gave surprising results. Scientists predicted almost isothermal polar caps at about 145-148 K in vapor pressure equilibrium with the atmosphere. The Viking Infrared Thermal mapper (IRTM) which was expected to measure such surfaces temperatures with its 11-μm and 20-μm channels found considerable structure with minimum brightness temperatures far below the CO_2 frost point, often below 135 K (Kieffer *et al.*, 1977). The location and brightness temperatures of these anomalously "cold" areas were highly variable, sometimes on time scales of days. There were observed at most polar latitudes in the northern hemisphere unlike in the southern hemisphere where they were less frequent, especially equator-

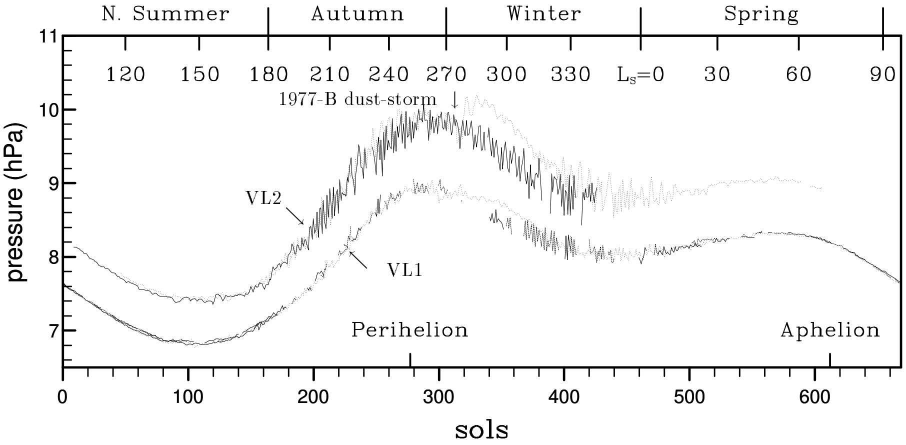

Figure 1. Time evolution of the surface pressure recorded by the two Viking landers during the first three Martian years: year 1 (dotted), 2 (solid) and 3 (dashed) are superimposed on the same graph. The large seasonal variation of the surface pressure are primarily due to the condensation of the atmospheric CO_2 in the seasonal polar caps. Figure from Hourdin *et al.* (1993), data from Tillman and Guest (1987).

ward of 80^{o}S (Forget and Pollack, 1996, Kieffer *et al.*, 1977) . In particular, an exceptionally high frequency of occurrence of extremely low brightness temperatures was reached near the north pole right after the first phase of the second global dust storm observed by Viking, a few days after the northern winter solstice.

The Mariner 9 IRIS spectrometer polar night observations - analysed only recently by Paige *et al.* (1990a) - show that these areas exhibit a complex spectral signature (Fig.2), at least in the northern polar region in late winter (the only period and region for which relevant IRIS spectra are available).

Hypotheses for explaining these observations include a strong enrichment in lighter, non-condensible gases in the winter polar atmosphere allowing the partial pressure of CO_2 to be less than that at low latitude (Kieffer *et al.*, 1977) , low surface emissivities for carbon dioxide frost (Ditteon and Kieffer, 1979), and the presence of carbon dioxide clouds (Hunt, 1980). Hess (1979) cast doubt on the feasibility of the noncondensible gas enrichment by showing that vertical and horizontal gradients in the average molecular weight of the Martian polar atmosphere could be stable only under very special circumstances. The last two hypotheses have been supported or studied by various authors. They are reviewed in the next two subsections.

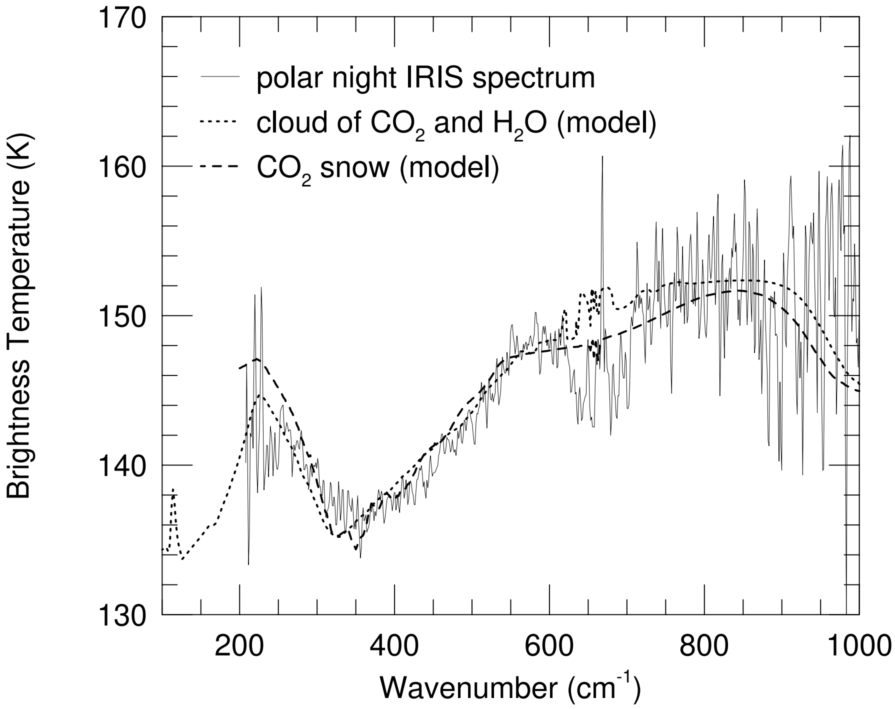

Figure 2. Typical Mariner 9 IRIS spectrum of the northern polar cap during the polar night (75°N,150°W, $L_s = 331°$). Data below 225 cm^{-1} and above 750 cm^{-1} are very noisy and thus not reliable. The prominent feature extending from about 600 to 800 cm^{-1} is due to absorption and emission by gaseous CO_2. Outside the CO_2 gas band, the spectra can be matched by simulated spectra of precipitating CO_2 cloud ($r = 50\mu$m) mixed with water ice particles (dotted line) as well as simulated spectra of CO_2 snow ($r = 2.5$-mm) contaminated by 0.05 % of dust and 0.05 % of water ice (dashed line). Figure from Forget *et al.*, 1995.

2.1.1. *Radiative properties of the CO2 frost in the thermal infrared*

Most natural planetary surfaces have emissivities above 90% in the thermal infrared. In particular snow and sea-ice on Earth always have emissivities near 99% (Warren *et al.*, 1990). However, CO_2 ice has the property that its interband absorption in the infrared is much smaller than, for example, that of H_2O ice. This is apparently due to the lack of hydrogen-bonding in CO_2 ice (Warren, 1986). The interband absorptions were first measured in the laboratory by Ditteon and Kieffer (1979) who suggested that CO_2 snowflakes and frost could be efficient scatterers and thus have a low emissivity. Recent accurate laboratory measurements by Hansen (1993) indicate that in the spectral regions on either side of the strong 15μm absorption, the CO_2 ice is actually a factor of ten more transparent than reported by Ditteon and Kieffer. Using such laboratory data, the emissivity of pure

CO_2 ice deposits can be estimated using radiative transfer models (Warren *et al.*, 1990; Forget *et al.*, 1995). These models have confirmed that Martian CO_2 frost could theoretically have an emissivity much lower than one in the thermal infrared. At any wavelength the primary variable controlling the radiative transfer properties is the snow grain size: the emissivity strongly increases with grain size. Contamination by dust and especially water ice can also raise the emissivity especially near their respective absorption bands. The emissivity could also depend on other properties not accounted for in the models, such as the grain shape. For instance, it seems reasonable that, if the growth can proceed in alternative ways, the form which maximizes the emissivity will be favored since such particles will cool, and grow at the maximum rate (James *et al.*, 1992).

On Mars, outside the observed anomalously low brightness temperatures areas, and especially in early fall, late winter and spring where no specific spectral signature was detected, the Martian polar cap emissivity is likely to be high (Paige, 1985; Forget *et al.*, 1995). According to the models, that would require very large grain sizes, or more precisely spectroscopic path lengths on the orders of centimeters. Water ice and dust contamination could help but unrealitic amounts would be required to raise the emissivity above 0.9 (Warren *et al.*, 1990). Large spectroscopic path lengths are also suggested by near-infrared observations of the subliming cap (section 3.1.3) and implications are discussed in section 3.2.

Can the low brightness temperatures be explained by spatial variations in surface emissivity ? The observed spectral features in the IRIS and IRTM data can be reproduced by modeled millimeter sized grains CO_2 snow deposits mixed with small amounts of water or dust (Fig. 2; Forget *et al.*, 1995). The high spatial and temporal variability of the brightness temperatures would suggest a scenario based on the different properties of CO_2 snow originating from the atmosphere and ice formed on the ground, as explained below.

2.1.2. *Carbon dioxide ice clouds and snow*

As first suggested by Gierash and Goody (1968) , further studied by Paige (1985) using a one-dimensional polar radiative model, and more recently modeled and analyzed with an atmospheric General Circulation Model (Pollack *et al.*, 1990), atmospheric CO_2 condensation could occur at most altitudes in high latitudes during the fall and winter seasons. CO_2 ice particles are likely to form clouds in the polar night atmosphere.

Only limited observational evidence of CO_2 clouds exists. Clouds in the polar regions of Mars have been known for decades, especially in the northern hemisphere, and are referred to as “polar hoods” (see Briggs and Leovy, 1974; Briggs *et al.*, 1977) , but Mariner 9 IRIS showed that the northern winter hood was composed of water ice, at least south of 65°N. However, Briggs and Leovy (1974) observed at higher latitudes some cloud lines formed at the CO_2 ice temperature, with very distinct fine structure. They showed that water ice clouds could not have exhibited such structure because of the slow condensation and sublimation rates of water ice at low temperature, and that these clouds were likely to be composed of CO_2 ice. Also, three of the Mariner 6 and 7 infrared spectrometers limb spectra have been interpreted as a reflection on thin CO_2 clouds because of characteristic spikes at 4.26 μm (Herr and Pimentel, 1970).

Kieffer *et al.* (1976) first suggested that CO_2 clouds could create the anomalously low IRTM brightness temperatures, among other possibilities. Pollack *et al.* (1990) showed that the spatial and temporal variabilities of the modeled atmospheric condensation rate were consistent with those exhibited by the low 20-μm brightness temperatures mapped by the Viking IRTM. In particular, the fact that the second Viking dust storm was followed by a period of maximum frequency and intensity of low brightness temperature events is consistent with model results: by its radiative effect, dust strongly increases the atmospheric emissivity, its cooling rate, and thus the atmospheric condensation rate (Pollack *et al.*, 1990). Model calculations indicate that increasing the dust optical depth from 0 to 5 in the winter polar atmosphere produces a transition from a situation in which almost all the carbon dioxide condenses on the ground to one in which it nearly all condenses in the atmosphere. It also seems likely that the dust particles can serve as cloud condensation nuclei, along with H_2O ice particles.

CO_2 ice clouds are expected to affect the infrared emission of the polar caps mainly by scattering the radiation emitted by the surface back to the surface, if their particles are not too small (Hunt, 1980; Forget *et al.*, 1995). Non-precipitating CO_2 clouds, composed of particles smaller than a few micrometers should be transparent in the infrared, whereas precipitating CO_2 clouds with particle radii larger than 10-μm should effectively scatter the infrared radiation. The hypothesis of opaque CO_2 clouds emitting higher in the atmosphere in a colder layer (Paige *et al.*, 1990a) seems to be incompatible with the observations (Forget *et al.*, 1995).

As for the CO_2 ice deposits, such clouds are able to produce the observed infrared features if the CO_2 ice particles are mixed with small amounts of water or dust (Fig. 2; Forget *et al.*, 1995). In fact, the signature of CO_2 ice clouds and deposits are rather similar in that they both rely on the fact that intermediate size CO_2 ice grains can be efficient scatterers at infrared wavelengths, whether they are airborne or on the ground. CO_2 ice deposits composed of much larger grains or nonporous solid ice having directly condensed on the ground or having undergone frost metamorphism should have an emissivity close to unity, and, in any case, much higher than that of small CO_2 ice particles originating from atmospheric condensation. Besides, if the solid CO_2 ice layer is thin enough, it is likely that it will be transparent in the infrared and that the ground beneath will radiate through (with a high emissivity). On the basis of these results, Forget *et al.* (1995) suggested that the low brightness temperatures were likely to be created by CO_2 snow falls, and that both falling snow particles and fresh snow deposits could contribute to create the observed features.

2.2. ENERGY BALANCE AND MODELING OF THE CONDENSING POLAR CAPS

Because actual observations are limited, significant advances in our understanding of the formation of the seasonal polar caps have been obtained through thermal balance modeling. The amount of CO_2 which condenses in the polar caps is controlled by the energy balance of the Martian polar regions: the total net flux of energy into a region at its boundaries must be equal to the rate at which energy is stored inside the region. Since condensation can occur both in the atmosphere and on the surface, the combined atmosphere + surface column energy balance equation must be considered. To first order, it gives

$$C_{CO_2} = [F_{IR}^{\uparrow} - Adv - Cond - (1 - A)F_{solar}^{\downarrow}]/L \tag{1}$$

where C_{CO_2} is the total CO_2 condensation rate (kg m^{-2} s^{-1}); L the latent heat of CO_2 (5.9×10^5 J kg^{-1}); $F_{IR}^{\uparrow}$ the thermal infrared flux of the system toward space; Adv the heating rate due to heat transport by the atmosphere to the system (advection); $Cond$ the subsurface heat conduction flux (positive when the subsurface is warmer than the surface); A is the planetary albedo at solar wavelengths; $F_{solar}^{\downarrow}$ the solar flux at the top of the atmosphere. This last term is of course equal to zero at night and especially during the polar night, when most of the condensation occurs.

Outgoing infrared emission: Under regular conditions (i.e. outside the dust storm period), the thermal infrared flux toward space $F_{IR}^{\uparrow}$ is usually the major term (Pollack *et al.*, 1990; Hourdin *et al.*, 1995). It can be determined from spacecraft observations. In particular, the Viking IRTM observations have been used to determine the seasonal evolutions of $F_{IR}^{\uparrow}$ during the first Viking year for the core regions of the residual cap (Paige and Ingersoll, 1985), and more recently for the entire seasonal caps during the polar night seasons (Forget and Pollack, 1996). $F_{IR}^{\uparrow}$ was primarily affected by the low brightness temperatures events described in Section 2.1, especially in the northern atmosphere (Forget and Pollack, 1996).

Polar caps surface temperatures and thermal emission: When the atmosphere is clear, $F_{IR}^{\uparrow}$ is usually close to the infrared flux emitted by the surface. In models, this flux can be computed as $F_{surf\uparrow} = \epsilon\sigma T_{surf}^4$, with σ, the Steffan-Boltzmann constant (5.67 10^{-8}), ϵ the spectrally averaged emissivity and T_{surf} the surface temperature. The CO_2 ice surface temperature T_{surf} only depends on the local atmospheric pressure p, through the CO_2 vapor pressure curve: $T = 3148/(23.102 - \ln p)$ with T in Kelvin and p in millibars (see James *et al.*, 1992). In spite of this relation, the cap surface temperatures are poorly known because of the large uncertainties in the available Martian topographic data used to derive the surface pressure. This is a serious obstacle to modeling and understanding the physics of the caps. Estimating directly the ground ice temperatures from infrared observations is difficult because of the anomalous brightness temperature observed during the polar night and because of the strong emission of the dust particles warmer than the surface cap when the atmosphere is sunlit. Actual "thermodynamic" ground ice temperatures have been estimated at the pole by Paige and Ingersoll (1985), and more recently mapped for the global polar caps by Forget and Pollack (1996). Interestingly enough, these temperatures seems to be colder than the expected frost point of CO_2 for the topography of the polar regions which is usually used in the models. In both hemispheres, there is an apparent systematic decrease of the temperature toward the pole, but the southern polar cap is globally 4 K colder than the northern cap. Near winter solstice, temperatures at the pole are about 145.5 K in the north and 141.5 K in the south, corresponding to pressures of respectively 4.3 mbar and 2.3 mbar.

Atmospheric radiative effects: $F_{IR}^{\uparrow}$ can be affected by the presence of other aerosols such as airborne water ice or dust, and by the absorption and emission of the gaseous atmosphere in the 15-μm band. In the southern hemisphere, model results (Pollack *et al.*, 1990; Hourdin *et al.*, 1995) and available infrared observations (Martin and Kieffer, 1979; Martin, 1981) suggest that the winter polar atmosphere is approximately isothermal. Its net effect on the total outgoing radiation should thus be negligible. This is not valid for the northern fall and winter seasons observed by Viking during which two global dust storms occurred. The second storm caused a strong increase of the infrared emission measured by all the IRTM channels, especially in the 9-μm and 11-μm channel. This dust storm warming was particularly strong near the cap edge. It decreased with latitudes but was still observable in the polar region (Martin, 1981). This second storm, and to a lesser extent the first one were accompanied by a more durable and particularly intense warming of the upper atmosphere in high northern latitudes thought to be caused by complex atmospheric dynamical processes

(Martin and Kieffer, 1979; Jakosky and Martin, 1987). Despite the fact that the clear upper Martian atmosphere only radiates in the the 15-μm gaseous CO_2 band, this polar warming considerably increased the total infrared emission toward space of the polar regions (Forget and Pollack, 1996).

Atmospheric heat advection: During the dust storms, the strong increase of the infrared emission toward space $F_{IR}^{\uparrow}$ does not imply that more CO_2 condensed during these periods: this increase is nothing but the observable consequence of a much larger advection of energy toward the pole by the atmosphere. In equation 1, the observed increase of $F_{IR}^{\uparrow}$ was certainly correlated with a much larger increase of Adv, causing the CO_2 condensation to decrease or even stop during these periods (Martin and Kieffer, 1979). The heat advected above the caps during the upper atmosphere polar warming events only directly affects atmospheric levels located above the expected level of condensation but it inhibits the condensation rate indirectly by its radiative effect (Martin and Kieffer, 1979; Forget and Pollack, 1996).

More generally, theoretical studies conducted with atmospheric general circulation models (Pollack *et al.*, 1990; Hourdin *et al.*, 1995) confirm that the heat advection by the atmosphere Adv plays a fundamental role near the cap edge (up to 20-30 Wm^{-2}), especially for enhanced dust loading. This role is probably much smaller near the center of the seasonal cap (a few Wm^{-2}) , as suggested by the heat budget studies by Paige and Ingersoll (1985).

Subsurface heat conduction: The subsurface conduction $Cond$ accounts for the energy stored in the subsurface material during the year. Thus, it is positive and non negligible, especially when the caps start condensing, and where the thermal inertia is high. Actual values of the subsurface thermal inertia are poorly known below the diurnal skin depth on Mars. This uncertainty must be taken into account when modeling the polar caps (Wood and Paige, 1992). The highest thermal inertia should be found on the water ice north residual cap, where the subsurface conduction could reach 20-30 Wm^{-2} (Paige and Ingersoll, 1985). On the other hand, $Cond$ is probably close to zero on the south residual cap where the temperature is constant all year long. This difference between the North and South caps may be important in explaining the polar caps asymmetry (Jakosky and Haberle, 1990).

Application: polar cap models. Since Leighton and Murray (1966), many models have been developed to simulate the formation of the Martian polar caps by examining their energy balance (e.g. Briggs, 1974; Davies *et al.*, 1977; James and North, 1982; Wood and Paige 1992; Pollack *et al.*, 1990, 1993; Hourdin *et al.*, 1993, 1995). Most recent models are able to reproduce the annual variations in atmospheric pressure shown in Fig 1, but most studies concluded that it was necessary to use artificially low values for the modeled caps emissivities to account for a condensation rate lower than expected. This confirms that in these models major processes have not yet been taken into account or properly treated (e.g. CO_2 clouds and snow, heat advection during the dust storm, upper atmosphere polar warming) and that the available datasets used for the topography and for the seasonal thermal inertia may not be accurate.

2.3. EXTENSION, MASS AND THICKNESS OF THE POLAR CAPS

Extension: The locations of the polar caps boundaries during their condensation phases and their maximum extensions are not very well known for several reasons. First, since during the fall and winter seasons, Martian poles are by definition tilted away from the Sun -and thus from Earth-, telescopic observations have been difficult to obtain. Moreover both spacecraft and telescopic observations in the visible are complicated by the near coincidence of the terminator with the edge of the cap. Nevertheless, Viking observations of the south polar cap (Briggs *et al.*, 1977; James *et al.*, 1983) confirm terrestrial observations that the surface frost extends to between -50^o and -55^o latitude and reaches as far north as -40^o latitude in the relatively low-elevation Hellas and Argyre basins which are covered preferentially by the frost as expected from energy balance consideration (Low elevations have higher pressures, corresponding to higher frost formation temperatures).

In the northern hemisphere, observations of the cap boundaries are even more difficult. These regions are usually obscured by clouds during fall, winter and early spring to latitudes as low as +40^o. These clouds, generally referred to as "polar hood", have been studied for decades by telescopic observers who were able to distinguish them from the ground ice because of their high variability and their higher opacity in images obtained with blue and violet filters. The polar hood has also been observed in details by Mariner 9 and Viking (Briggs and Leovy, 1974; Briggs *et al.*, 1977). The camera aboard Mariner 9 showed that the hood is diffuse at latitude higher than 60^o, but that it exhibits complex wave structures at lower latitudes. A southern polar hood also exists but is much less prevalent than the northern one (James *et al.*, 1979).

Analysis of images of the north polar cap acquired with various filters from Earth (e.g. James *et al.*, 1987) and by Viking (James, 1979; 1982) suggest that the cap extends to roughly 55^o in late winter. This is supported by the IRTM data analyzed by Christensen and Zurek (1984).

During the late fall and winter seasons, the second Viking Lander located at 48°N latitude observed thin surface frost deposits (Jones *et al.*, 1979; Wall, 1981). There has been considerable debate about whether the frost was composed of CO_2 or H_2O ice, although the most recent studies have favored a H_2O ice composition (Hart and Jakosky, 1986; Svitek and Murray, 1990).

Mass: The mass of the polar caps cannot be observed remotely, although future gamma-ray spectrometers could come close by measuring remotely the effect of the CO_2 on the gamma-ray and neutron emissions. Nevertheless, the amount of CO_2 which gets globally trapped in the seasonal polar caps can be estimated from the seasonal surface pressure variations measured by the Viking Landers (Fig. 1). This is not straightforward, since these variations are not only due to condensation and sublimation of atmospheric carbon dioxide in the polar caps, but are also strongly influenced by internal mass redistribution associated with the atmospheric circulation (Talagrand *et al.*, 1991; Hourdin *et al.*, 1993; Pollack *et al.*, 1993). For this reason, the surface pressure cycle depends on the location on the planet and is not simply related to the global atmospheric mass cycle. Hourdin *et al.* (1995) used a global circulation model to estimate the local meteorological component and thus the global atmospheric mass budget from the Viking data, with a rather good accuracy except for the fact that global Martian topography is not very well known. Corresponding model results showed that for a consistent total seasonal cap + atmospheric carbon dioxide budget of about 6.8 mbar, an equivalent pressure up to 1.0 mbar and 1.7 mbar gets trapped every year in the north and south polar cap respectively.

Thickness: The thickness of the CO_2 ice layer is thought to be highly variable (James *et al.*, 1979): as explained above, the local condensation and sublimation rate depends on latitude and on the local topography, winds, and surface properties. Wind redistribution also plays a significant effect, for instance accumulating frost in the lee of craters (Thomas *et al.*, 1979). Using the Viking IRTM data to determine annual radiation budget and infer the annual carbon dioxide frost budget of the Martian north and south residual cap regions, Paige and Ingersoll (1985) calculated that during the winters observed by Viking, there was about 75 g cm^{-2} of CO_2 frost deposited at the north pole and about 110 g cm^{-2} deposited at the south pole. This corresponds to maximum cap thickness of the order of 0.5 and 0.7 m, respectively, in the fully dense state ($\sim$1.6 g cm^{-3}). Such results are consistent with most polar cap models, including the pioneering works by Leighton and Murray (1966) and more recent and sophisticated models (e.g. Hourdin *et al.*, 1995). Thomas *et al.* estimated that the maximum winter accumulation of frost in some observed frost streaks lying in the lee of craters was of the order of 100-150 g cm^{-2}.

3. The subliming Martian Polar caps

3.1. SPACECRAFT AND TELESCOPIC OBSERVATIONS

3.1.1. *North Polar Cap*

The spring north polar cap has not been observed in detail for several reasons. First, the north polar hood clouds usually shroud the high northern latitudes during the first part of the spring. Second, only limited synoptic imaging by spacecraft is available, since spacecraft orbits imposed a limited areal coverage for Viking Orbiter 2 and undesirably large emission angles for Orbiter 1. Third, terrestrial observations must be acquired during aphelic oppositions when Mars is relatively small in diameter.

Nevertheless, there have been many studies focussing on the shape of the cap during recession and on the latitude of the cap edge. These include spacecraft visual imaging data (James, 1979; James, 1982), infrared data (Christensen and Zurek, 1984) and telescopic data (see recent publications by Iwisaki *et al.*, 1982; James *et al.*, 1987; James *et al.*, 1994). These observations indicate that during its recession, the north polar cap remains roughly circular and centered on the geographic pole. The cap edge usually "pauses" during at least 60 Martian days at about 65^o latitude during mid-spring (from roughly L_s = 20^o to L_s = 50^o). Interestingly enough, water ice clouds seem to be absent during the "standstill" but reappear when the recession resumes, suggesting that they are associated with water vapor released at the edge of the cap (James *et al.*, 1987). By the beginning of the summer, the CO_2 north polar cap completely sublimes exposing an underlying water ice cap which acts as a source for atmospheric water vapor.

3.1.2. *South Polar Cap*

Since the south pole is tilted toward Earth during favorable oppositions, there are relatively high quality data from terrestrial observations for the subliming south polar cap. Moreover, the 1977 spring and summer south polar cap of Mars was monitored in detail by Viking Orbiter 2 (James *et al.*, 1979; Thomas *et al.*, 1979) and the 1972 summer cap by Mariner 9. Viking picture mosaics are shown in Figures 3, 4 5, 6.

During the first part of the spring (until $\sim L_s = 240^o$), the perimeter of the cap is roughly circular and centered on the pole (Fig. 3; James *et al.*, 1979). The cap seems to have an annular structure with a bright periphery surrounding a darker ring which itself encircles a very bright central area: the residual cap, which can almost be distinguished "through"

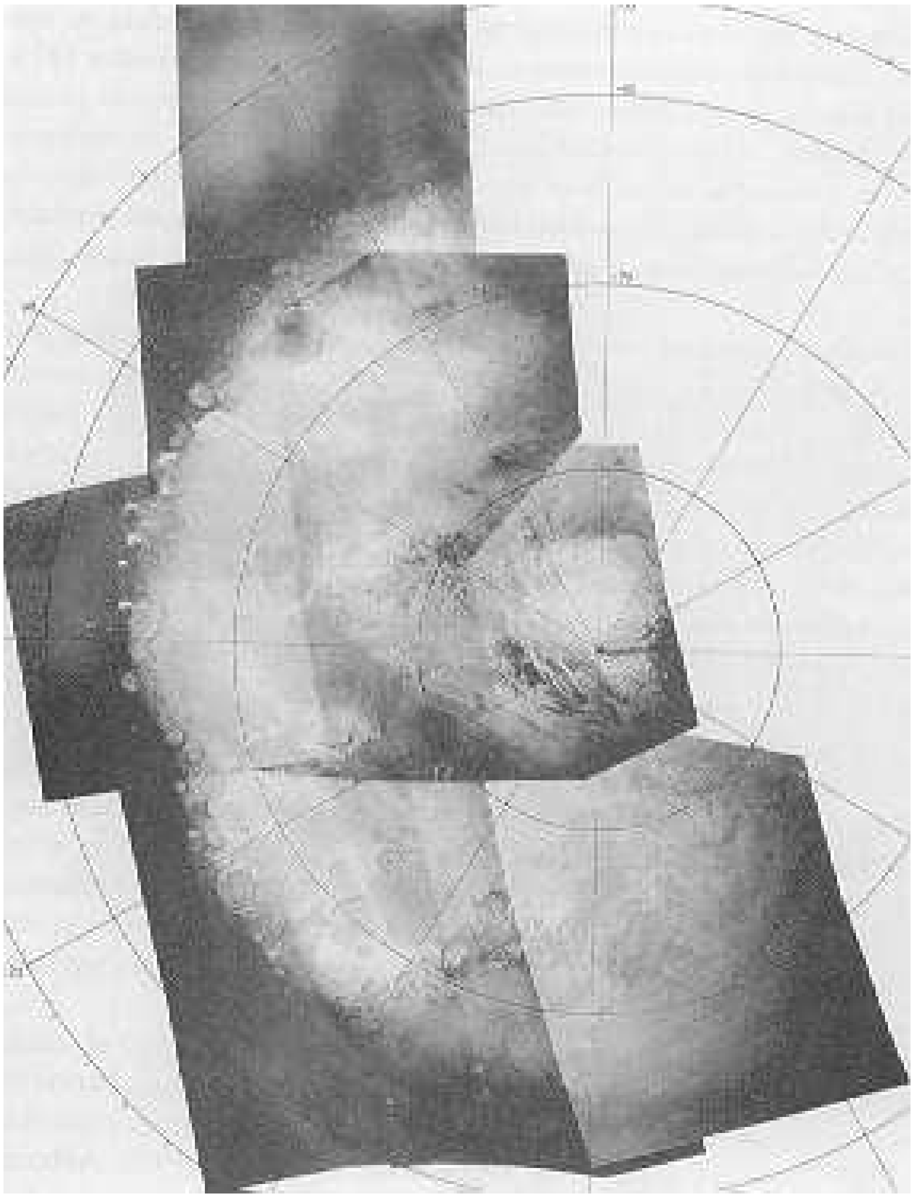

Figure 3. The south polar cap observed by Viking in midspring ($L_s = 221°$) The spring polar cap is characterized by small scale inhomogeneities in the polar cap boundary and in the albedos within the frost-covered region. These inhomogeneities have been observed to be reproducible on an annual basis, indicating that fixed topography or other surface properties control their appearance, either directly or through topographic control of winds (see Thomas *et al.*, 1979). In particular, many craters bottoms appear either brighter or darker than their surroundings and many of the bright outliers along the cap edge are found to be also in the bottoms of craters. The bright area near the pole is the south residual cap. Figure from James *et al.*(1979).

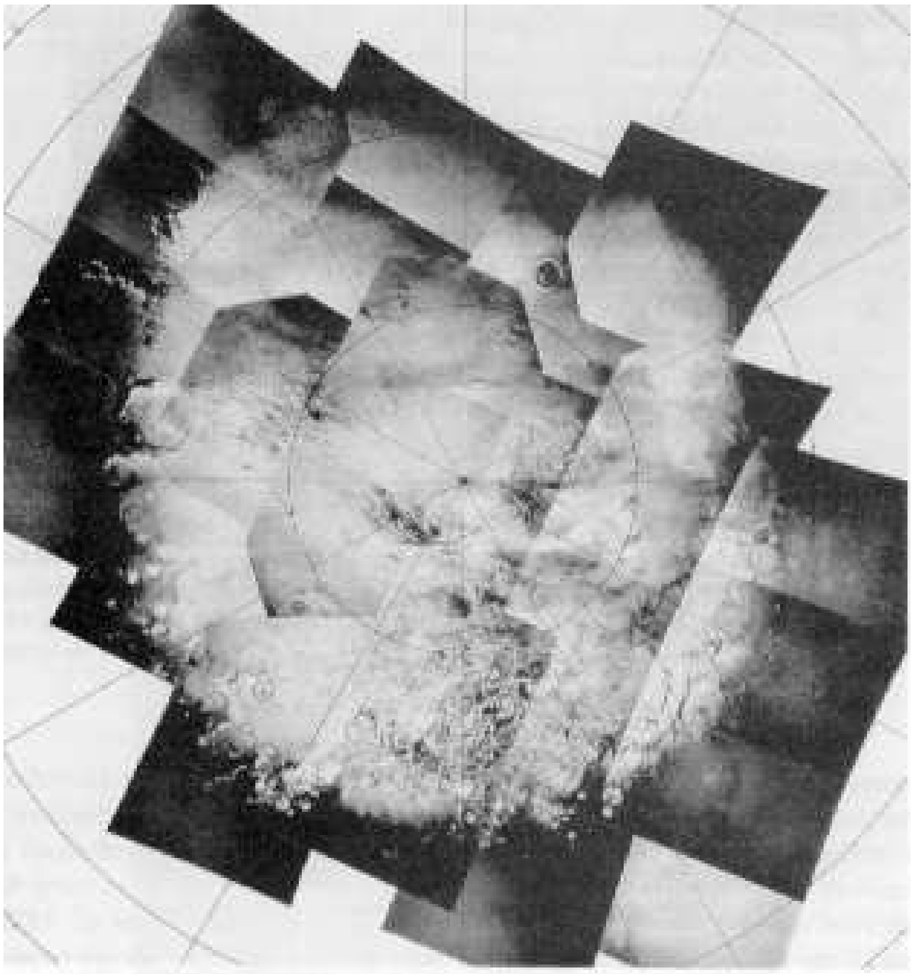

Figure 4. A view of the entire south polar cap obtained 27 days after the one shown in Fig. 3 ($L_s = 237°$). Large regions between 150°W and 300°W were already free of surface frost, forecasting the large asymmetry of the subsequent recession. (James *et al.*, 1979)

the seasonal frost. The annular structure seems to persist as the cap recedes, suggesting that resurfacing is involved (see section 3.4 about CO_2 frost albedo). During the second part of the spring, the frost between 160^o and 300^o longitude rapidly sublimes (Fig. 4), leading to a very asymmetric cap which, by southern summer solstice, results in a cap center displaced by 6.5^o from the geographic pole (Fig. 5).

After summer solstice, the cap keeps on shrinking slowly and by mid-summer remains a relatively small residual cap (Fig. 6). Then most of the changes are in detail rather than in the area covered by ice. Both Mariner

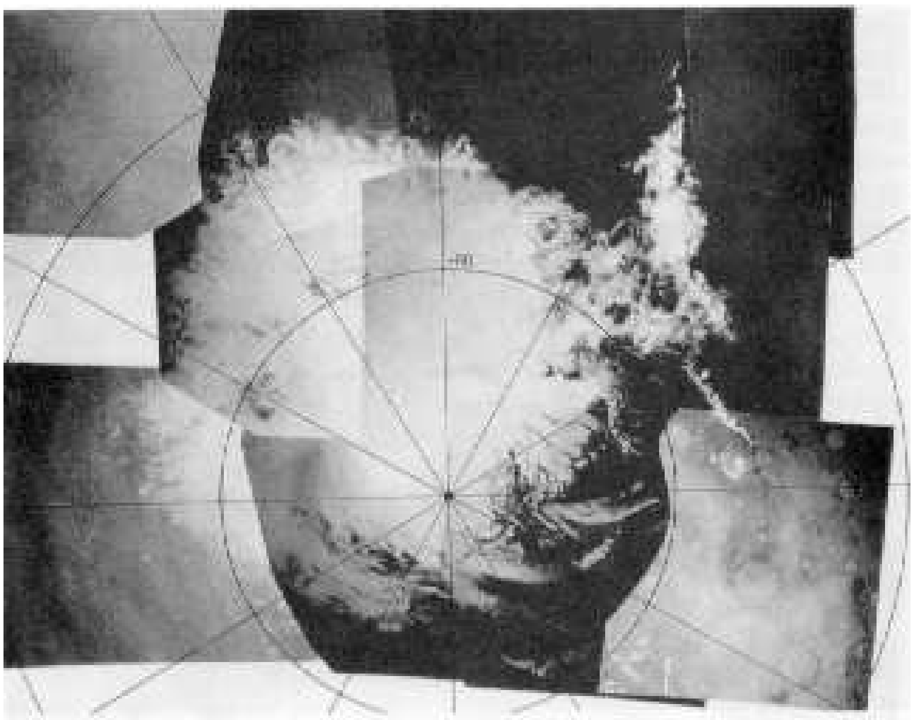

Figure 5. Shortly before summer solstice, ($L_s = 263°$), the south polar cap is unsymmetric and its center is displaced by about 6° from the pole. The "Mountains of Mitchel" which in early spring form a well known feature brighter than its surrounding has become a very obvious peninsula detached from the main cap near 320°W. (James *et al.*, 1979). The nomenclature "Mountains of Mitchel" is not official since the feature does not appear to be mountainous !

9 (Paige *et al.*, 1990b) and Viking (Kieffer, 1979) thermal infrared observations showed that, at least in 1971 and 1977, carbon dioxide survived all year long on the south residual cap. This behavior is surprisingly different from what has been observed in the north where CO_2 completely sublimes by the beginning of summer. Such a difference cannot be explained straightforwardly by the orbital asymmetry or a topographic difference. It is a major Martian curiosity which is addressed in section 3.3.

3.1.3. *Near Infrared Observations*

Telescopic and spacecraft near-infrared spectral observations have confirmed that the seasonal caps are mainly composed of CO_2. The Mariner 7 infrared spectrometer experiment first provided some spectroscopic evidence: Herr and Pimentel (1969) identified two diagnostic absorptions near 3.0 and 3.3 μm and cautiously concluded that a solid CO_2 composition "must

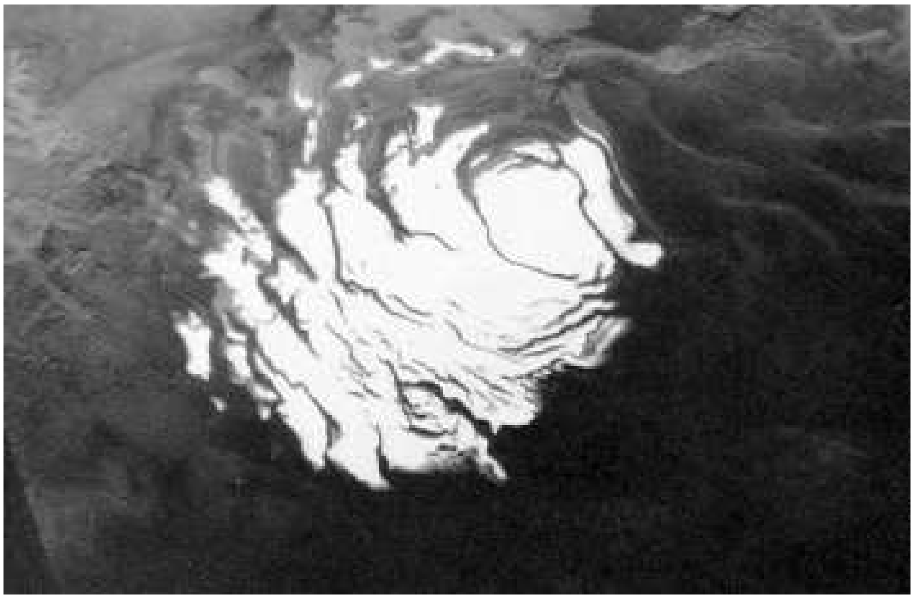

Figure 6. The south residual cap observed by Viking ($L_s = 341^o$). It is approximately 400 km accross. The frost outlier at the top of the picture survived the Viking year but not the year of Mariner 9. (James *et al.*, 1979).

be preferred". Later, Kieffer (1970b) pointed out that absorptions at 2.28 and 2.34 μm were characteristic of spin forbidden transitions in solid CO_2 but the features were not identified in the Mariner 7 data until 1974 (Pimentel *et al.*, 1974). Meanwhile, using an Earth-based high-spectral resolution Fourier spectrometer, Larson and Fink (1972) confirmed the CO_2 identification based upon 11 absorption features including the 2.28 and 2.34 μm transitions and other features near 1.2, 1.5-1.65 and 2.05 μm. Water ice was also observed on or above (clouds) the north polar ice cap, although interpreting these observations appears not to be straightforward (Kieffer, 1970a; Clark and McCord, 1982; Jakosky, 1983; Bell and Crisp, 1993).

Unfortunately, besides the data obtained during the Mariner 7 flyby of Mars in 1969, no spacecraft data are available since neither Viking nor Mariner 9 carried a near infrared spectrometer and since Phobos 2 did not observe the high Martian latitudes. Mariner 7 provided 25 spectra of the early spring south polar cap ($L_s = 200^o$) using wavelengths from 1.9 to 14.4 μm (Herr and Pimentel, 1969). This dataset was recently reanalyzed by Calvin (1990) and Calvin and Martin (1994). Using the accurate optical constants for solid CO_2 measured by Hansen (1992), Calvin and Martin (1994) modeled the spatial variability of CO_2 grain size and water

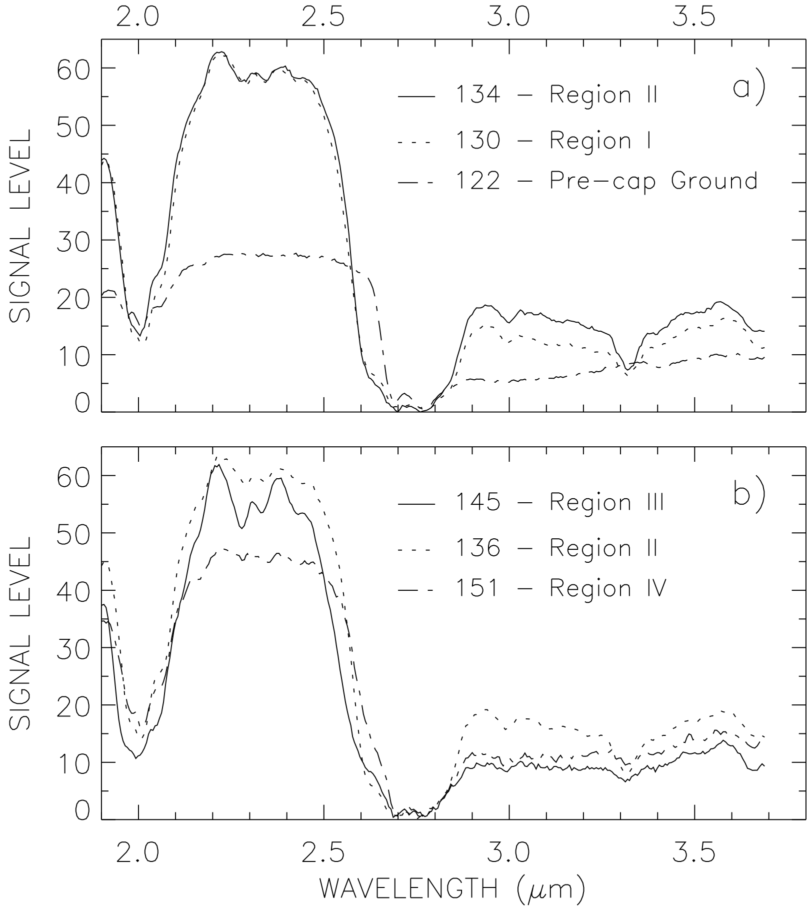

Figure 7. Selected spring south polar cap spectra measured by Mariner 7 ($L_s = 200^o$). Region I is at the cap edge, where there is enhanced water ice absorption beyond 3μm, inferred to be caused by increased sublimation rates. Region II is the typical cap interior. Region III is an anomalous region discovered near South Crater. Its unique spectral characteristics could be caused by increased path length in the CO_2 ice but theoretical models are unable to accurately reproduce the spectrum. Region IV is an area of thinning frost coverage or transparent ice well in the interior of the seasonal cap (Combination of CO_2 and ground signatures). Figure from Calvin and Martin (1994).

ice abundance. They discussed in detail the 2.28 and 2.34 μm features and their implications for the surface physical properties. They estimated that there was very little dust and some water ice at the level of a few parts per thousand. Equivalent grain sizes in simulated ices were surprisingly large, on the order of millimeters to several centimeters. Spatial variations were observed. They are described in Figure 7.

3.2. MICROPHYSICAL STATE OF THE CO_2 FROST

Both thermal infrared (Forget *et al.*, 1995) and near infrared (Calvin and Martin, 1994) observations of the Martian polar caps suggest that the spectroscopic "grain sizes" of the spring CO_2 snow could be larger than several centimeters. The seasonal cap in spring may be more like glacier ice containing cracks and bubbles, rather than a snow pack with individual grains (Calvin and Martin, 1994). Such large textural scales have also been found for the N_2 ice deposits on Triton. Eluszkiewicz (1993, chapter x, this book) has examined the microphysical process involved in frost condensation and metamorphism. On Mars, like on Triton, the atmosphere condenses in the near absence of an inert gas and the frost temperature is nearly constant. Thus no "air bubbles" and no thermal cracking are expected. Over the winter, the Martian CO_2 snow could undergo seasonal densification and sintering into a "nonporous, polycrystalline" layer, provided freshly condensed grains are sufficiently small. Such a layer could be slightly transparent. That could explain why the southern residual cap can be distinguished when the seasonal frost is present.

3.3. ENERGY BALANCE OF THE SUBLIMING AND RESIDUAL POLAR CAPS

Similarly to the condensation rate, the sublimation rate of the CO_2 ice frost is controlled by the energy balance of the polar regions. However, the sublimation phase is different since it only occurs at the polar cap surface. To first order, equation 1 in section 2.2 remains valid, although the subliming rate C_{CO_2} will be negative. The net solar flux $(1-A)F^{\downarrow}_{solar}$ is of course no longer negligible.

Insolation: The radiative fluxes during the spring and summer seasons are much stronger than during the winter. Therefore, the mass exchange during the sublimation phase is controlled by the local radiative balance. $F^{\downarrow}_{solar}$ is now the key parameter of this balance. It primarily depends upon the local incidence angle, which in turn depends upon the solar longitude L_s and the latitude (and locally upon the local slope). Because of the large eccentricity of the Martian orbit, the maximum flux $F^{\downarrow}_{solar}$ at the south pole at summer solstice is 1.5 times higher than at the north pole. The planetary albedo A is clearly a crucial parameter of the radiative balance. It is highly variable in space and time and its variations are not very well understood. The frost albedo issue is reviewed in section 3.4.

Atmospheric radiative effect: Both $(1-A)F^{\downarrow}_{solar}$ and $F^{\uparrow}_{IR}$ may be affected by the presence of dust or water clouds in the spring and summer atmosphere. Airborne dust has a non trivial impact on the sublimation rate at sunlit latitudes. On the one hand, it decreases the amount of solar radiation reaching the surface by scaterring and absorbing at visible wavelengths. On the other hand, it increases the downward infrared fluxes because it raises the atmospheric emissivity and warms the atmosphere by absorbing the solar radiation. In equation 1, it raises $F^{\uparrow}_{IR}$, but it is likely to decrease the planetary albedo A if the surface albedo is high enough, as is expected on the polar caps. To first order, these competing radiative effects cancel one another during the spring season, although dust should slightly reduce the total radiative flux at the surface and thus the sublimation rate during the cap recession (Davies, 1979; Lindner, 1990). However, Pollack *et al.* (1990) found that the net effect of enhanced dust loading may be a slight increase of the sublimation rate because it enhances the atmospheric heat transport into the polar cap regions. The impact of water ice clouds is also not simple. Lindner (1990) showed that clouds usually reduce the net radiation flux which strikes the surface except for low solar incidence angle, a common situation at polar latitudes. The cloud could then scatter the solar flux down to the surface and increase the surface illumination.

Atmospheric heat advection: The atmospheric heat advection Adv has been studied theoretically with atmospheric models which have shown that it should play a much smaller role during the cap recession than during the condensation phase (Pollack *et al.*, 1990; Hourdin *et al.*, 1995). In fact, this is due to the much stronger intensities of the radiative fluxes during the spring and summer seasons.

Subsurface heat conduction: During the sublimation phase, the surface CO_2 frost remains at a temperature similar to the fall and winter temperatures. Not much heat should be left stored in the ground. Thus, the subsurface heat conduction $Cond$ is likely to remain positive and very small on average. (Paige and Ingersoll, 1985). However, it could be non negligible locally near the cap edge when contiguous regions are uncovered and warmed by the sun.

Energy balance of the residual south polar cap: During the year of Viking and Mariner 9 observations, CO_2 frost was stable at the south residual cap throughout the year, but was not stable at the north residual cap. This difference occurred in spite of the fact that both poles receive the same amount of annual insolation, and despite the higher elevation of the south residual polar cap compared to the northern cap, which should thus be more stable. (The lower polar cap radiates more energy in the infrared because its pressure and thus its frost temperature is higher). Most theoretical models simulating the energy balance of the polar caps have been unable to preserve CO_2 ice at the south pole and still obtain agreement with other observations.

Paige and Ingersoll (1985) used the solar reflectance and infrared emission measurements obtained by the Viking IRTM to study the radiative balance of the residual polar cap areas. They calculated the annual radiative budgets and infer the annual CO_2 frost budgets. They confirmed the stability of the CO_2 frost near the south pole and showed that the north-south difference was due to very asymmetric behavior during the spring sublimation phase. The CO_2 sublimation rates were then much smaller in the south than in the north, and this was due to the higher albedo of the south residual cap relative to the north cap. This difference in albedo, added to the difference in subsurface heat conduction - which is rather high on the residual north cap and close to zero on the south residual CO_2 cap where the temperature is constant all year long - (Jakosky and Haberle,1990) explains why the north and south residual polar caps are so different.

3.4. CO_2 FROST ALBEDO

The albedo of the Martian polar caps is characterized by strong spatial and temporal variations. Getting quantitative measurements and understanding the process which control these variations is crucial for energy balance considerations and to explain the caps appearance.

The radiative properties of pure CO_2 were reviewed by Warren (1986). New accurate measurements have been obtained recently by Hansen (1992). Warren *et al.* (1990) used a model originally developed for terrestrial snow to study the theoretical behavior of the CO_2 frost albedo. Pure CO_2 frost was calculated to have a high albedo at visible wavelengths, strongly decreasing with grain size (e.g. $\sim$0.8,0.6 and 0.4 for grain radii of 0.1 mm, 0.5 mm and 2.0 mm). Dust contamination should lower the albedo whereas H_2O ice contamination should only increase it slightly.

Spacecraft or telescopic observations of the Martian frost albedo are made difficult by the presence of dust or clouds in the atmosphere. Even small optical depths of dust could significantly lower the planetary albedo over a bright surface (Davies, 1979). Several authors have published measurements of the polar caps reflectivity from telescopic observations (Dollfus, 1965; Lumme, 1976; Lumme and James 1984; James *et al.*, 1994). Unfortunately, because of the very limited viewing geometries for the caps as seen from Earth, estimating a reliable albedo suitable for heat balance calculation (i.e. hemispherical albedo) is very difficult and model depen-

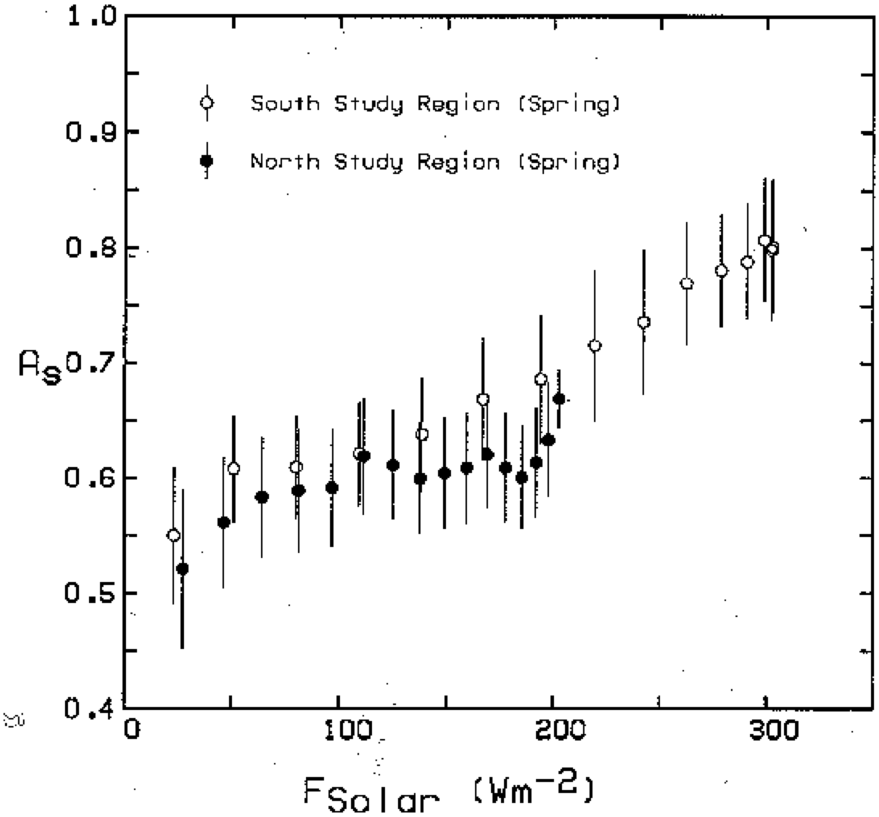

Figure 8. Estimated albedos of the CO_2 frost deposits within the vicinity of the residual cap regions shown as a function of the incident solar flux (Paige, 1985).

dent. Lumme and James (1984) estimates for the south cap in 1971 gave 0.64 at 360 nm (uv filter) and about 0.79 at 620 nm (red). Observations of the spring north polar cap with the Hubble Space Telescope gave values of 0.12-0.15 at 230-330 nm (uv), 0.34 at 413 nm (violet), 0.47 at 502 nm (green), and 0.73 at 673 nm (red) (James *et al.*, 1994). Similarly, Viking images were obtained through various filters and only included a limited range of viewing geometry. Photometric estimations for the bright portions of the seasonal polar cap led to albedos of 0.55-0.6 at 590 nm (red) and 0.36-0.38 at 440 nm (violet) (James *et al.*, 1979). These observations show that the Martian polar caps are reddish rather than white as would be expected for pure CO_2 or H_2O snow. This could be due to "red" dust contamination or maybe to the relative transparencies of the CO_2 frost layer so that the ground color is "viewed" through the frost (see section 3.2). James *et al.* (1979) found that the albedo of the residual south cap area was less dependent on wavelength (and usually higher than its surrounding).

The IRTM instrument aboard the Viking Orbiters made some calibrated, broadband (0.3-3 μm), solar reflectance measurements. The data obtained in the vicinity of both residual caps were studied in detail by Paige and Ingersoll (1985) and Paige (1985). In particular, they calculated the planetary albedo of these regions, and, using simple models, inferred the frost surface albedo. They found that it was approximately 25 percent lower in the north than in the south, and that it strongly varied through the summer, appearing to be nearly a linear function of insolation during this time, as seen in Fig. 8. The difference between the south and north spring residual cap albedo is usually attributed to a difference in dust contamination, linked with the seasonal dust cycle (Paige and Ingersoll, 1985). However, Fig. 8 suggests that it could be explained by Mars being closer to the sun during the southern spring and summer seasons.

The fact that the albedo could be an increasing function of insolation is not expected since it is the opposite of the relation for terrestrial frosts. In fact, the microphysical processes which control a CO_2 ice cap in vapor pressure equilibrium with the atmosphere are likely to be very different than on Earth. For instance, radiation incident on dust grains imbedded in a CO_2 frost will heat up the grains because of their low albedo. The solid CO_2 supporting the grain will sublime and the grain will sink into the frost or float away in the sublimation gas flow (Paige, 1985; James *et al.*, 1992). With such a process, the more insolation strikes the frost, the deeper the grains get, the brighter the surface becomes. Another specific process could be related to the fact that CO_2 ice is relatively "transparent" in the visible, more than in the thermal infrared (Warren *et al.*, 1986). Thus, the sunlight could be absorbed below the cap surface, deeper than where the infrared emission is emitted ("greenhouse effect"). Because the frost must be isothermal, the net energy balance will favor sublimation at the depth where the insolation is absorbed and the condensation nearer the surface where the infrared radiation is emitted. A strong insolation could result in the growth of pristine, high albedo frost deposits over a bulk deposit which would actually experience net sublimation (James *et al.*, 1990).

The seasonal south polar cap solar reflectance IRTM data were also discussed by Kieffer (1979) and are currently beeing reanalyzed by Ono and Paige (1995). Kieffer (1979) did not calculate hemispherical albedo but analyzed solar reflectances in term of Lambert albedo (reflectance normalized to that expected from an ideal diffuse white horizontal surface). In early spring, the Lambert albedo was found to decrease from ~ 0.5 near the cap edge to ~ 0.35 at -80^o latitude, before raising again in the residual cap area. Here again, a possible explanation for this annular structure could be a coupling between albedo and insolation.

3.5. INTERANNUAL VARIABILITY OF THE SEASONAL POLAR CAPS

The interannual variations in the observed seasonal polar caps could provide a measure of the degree of interannual variability within the Martian climate cycle. In particular, we have shown that the presence of dust and water ice is expected to affect the condensation and the sublimation phase of the caps through impact on the radiative properties of both the atmosphere and the cap surface, on the atmospheric circulation, and on the formation of CO_2 clouds and snow. Both the dust and the water cycle are thought to be highly variable from year to year on Mars. For instance, global dust storms such as the ones observed during the first Viking year do not occur every Martian year (Zurek and Martin, 1993) and in particular no dust storms were observed during the second and third Viking year.

South Polar Cap: James *et al.* (1987) reviewed the interannual variability of the Martian south polar cap recession for which data from many years are available. Several regressions, particularly the fast 1956 regression, were found to differ significantly from the mean. They explored the possibility of correlations with global dust storms and suggested that regressions associated with early spring storms may be slower than those that are not. However, summer global dust storms did not appear to have any systematic effect. The Mariner 9 and Viking missions permitted a detailed comparison of the summer phase of the south cap in 1972 and 1977 (James *et al.*, 1979). In spite of the fact that the spring regression curves were very similar (James and Lumme, 1982), the summer cap retreat observed by Viking was slower. The general behavior in 1977 was similar to that seen by Mariner 9, but delayed by several weeks. Several icy regions, including the cap outliers, survived the Viking year but totally sublimed in 1972.

North Polar Cap: In the northern hemisphere, less reliable data are available. Slight interannual differences were reported by Iwisaki *et al.* (1982) and Parker *et al.* (1983) but better data are probably needed to fully establish the existence and pattern of interannual fluctuations (James, 1979; James *et al.*, 1994).

Seasonal pressure variation: In spite of the theoretical and observational evidence for some interannual variability in the seasonal polar caps, the seasonal pressure variations recorded by the Viking Landers over several Martian years (Fig. 1) were almost perfectly repeatable (Tillman, 1988;

Paige and Wood, 1992). In particular, the pressure cycle, and thus the global CO_2 cap mass, was not significantly affected by the two global dust storms of the first Viking year. (The jump in pressure observed by VL2 during its first winter was caused by a dynamical effect related to the second Viking global dust storm; Hourdin *et al.*, 1993).

This puzzling repeatability suggests that dust and dust storms may not have a strong impact on the global polar energy balance, or, more likely that this impact was not very different during these three years. Except for the fact that no global dust storm occurred during the second Martian year, the "background" airborne dust underwent a strong seasonal cycle comparable to the first year cycle (Colburn *et al.*, 1989). Another - fascinating - explanation would be that the Martian CO_2 cycle is regulated by feedbacks which are still unknown.

4. Permanent CO_2 ice deposits ?

It has been shown that the residual south polar cap was covered by CO_2 ice at least when it was observed by spacecraft in 1972 and 1977 (Paige *et al.*, 1990b; Kieffer, 1979).

The existence of large amount of permanent CO_2 ice on Mars would have great significance for the Martian climate: If CO_2 ice remains at the pole all year long, the mean annual atmospheric pressure is controlled through vapor-pressure equilibrium by the mean annual CO_2 ice temperature, which, in turn, mainly depends upon the radiative balance of the polar region (Leighton and Murray, 1966). Such permanent CO_2 deposit would thus buffer or regulate the atmospheric pressure in response to changes in orbital parameters, especially obliquity, since the average insolation at the pole is proportional to the sine of the obliquity (see review by Kieffer and Zent, 1992). Recent calculations of the Martian obliquity suggest that it varies chaotically, ranging from about 0^o to 60^o in about 10^7 years (Laskar and Robutels, 1993). In theory, at low obliquities, a lower annual polar insolation results in an increase in permanent frost at the pole and a decrease in atmospheric CO_2 (Ward *et al.*, 1974). The system reaches a stable balance so that every year, the amount of CO_2 which condenses during the polar night is equal to the amount of CO_2 which sublimes during the sunlit seasons. Within this context, it is theoretically unlikely that both poles can keep a year round covering of CO_2 frost (Jakosky *et al.*, 1993). That would require both polar caps to have just the right combinations of albedo, emissivity, radiation temperatures, etc... to perfectly balance each other. One cap will be favored at the expense of the other. For example, if albedo and emissivity are the same, CO_2 frost will move preferentially to the lower cap, with a time scale much shorter than the orbital oscillations (Jakosky *et al.*, 1993). When the obliquity is high, the polar insolation can be too high to allow a limited cap + atmosphere CO_2 budget to keep both permanent CO_2 ice deposits at one pole and the corresponding high atmospheric pressure.

The current situation fits rather well within these theoretical considerations, which explains why there is a small permanent CO_2 ice cap at the south pole and not at the north pole. The fact that the south pole is currently favored is surprising at first glance because the south pole is higher than the north pole. This could be explained by the orbital eccentricity which affects the polar energy balance through seasonal asymmetries in insolation and airborne dust which in turn are thought to create the strong north-south polar albedo difference.

However, the capacity of a small south residual cap to actually buffer the Martian atmosphere depends on the amount of CO_2 currently stored in the south residual cap, which is unknown. It is a relatively small area and its thickness has not been estimated. A thickness of 1 to 100 m would correspond to 0.6% to 60% of the current atmospheric mass (Kieffer and Zent, 1992). This thickness could be variable from year to year. Comparison of 1972 (Mariner 9) and 1977 (Viking) images of the summer southern cap shows that the residual cap grew during this period (James, 1979). Besides, there is a possibility that CO_2 ice does not always survive at the south pole during summer. In particular, Earth-based measurements made in 1969 showed a factor of 6 more water during late southern hemisphere summer that was seen by Viking. Jakosky and Barker (1984) suggested that the south cap lost its CO_2 ice coverage exposing an underlying water ice residual cap similar to the northern one (The presence of a water-ice cap underlying the CO_2 frost at the south pole is expected because the CO2 ice acts as a cold trap for H_2O). However, alternative explanations exist. Rizk *et al.* (1995) computed that year-to-year variations in the amount of dust in the atmosphere could causes changes in the atmospheric dynamics and water vapor transport sufficient to explain the 1969 measurements.

Jakosky and Haberle (1990) modeled that the south cap could theoretically take two stable configurations at the current epoch: CO_2 frost can survive all year long, or sublime in early summer like in the northern hemisphere. The difference depends on the role of subsurface heat conduction: if the cap was exposed the previous year, conducted energy will cause less CO_2 frost to condense in winter, and the frost will disappear completely in summer; if the cap was covered the previous year, there will be no conducted energy, and it will stay covered again. Interannual variations affecting the local energy balance (see sections 2.2 and 3.3) could cause the cap to jump from one stable state to the other (Jakosky and Haberle, 1990).

The fact that the current permanent CO_2 cap could be small, thin or even absent some years suggests that the current Martian system is precisely at the limit between the low obliquity and the high obliquity scenarios described above. Could this be fortuitous? Jakosky and Haberle's results suggest that The jump between the permanent cap state to the other can occur for a wide range of cap + atmosphere CO_2 budget Therefore the range of obliquity during which both states may be found could be quite large, and thus the current situation is not that exceptional. In spite of the Jakosky and Barker (1984) observations, the possibility that a large amount of CO_2 ice (a reservoir from an earlier epoch) is currently being uncovered at the south pole cannot be ruled out. Future observations, such as measurements by gamma ray and neutron spectrometers will provide indications of the thickness of the CO_2 frost. Radar experiments recently performed from Earth by Butler *et al.* (1995) found a unique, highly reflective feature with a polarization inversion associated with the residual south cap, and no features associated with the north residual cap. Although the radar observations cannot tell if one is composed of thick CO_2 or H_2O, they concluded that such a difference was probably due to fundamental differences in the structure and/or composition (amount of cracks, voids, dust contaminants).

Other permanent CO_2 ice reservoirs could exist on Mars and contribute to the CO_2 cycle on long timescales. First, a large amount of CO_2 ice may be adsorbed in the regolith of the planet (see review in Kieffer and Zent, 1992) . If so, such a reservoir could buffer the entire atmosphere plus cap system, and could explain why the current CO_2 inventory is so close to the limit between permanent and non permanent CO_2 ice caps. Second, Jakosky *et al.* (1995) have recently suggested that large amounts of CO_2 ice (or CO_2-H_2O clathrate hydrate) could be buried beneath the water ice cap at both poles. If true, it would mean that the Martian climate could fluctuate wildly with the obliquity cycle (Haberle 1995).

5. Conclusion

Since the earliest spacecraft observations it has been known that the seasonal Martian polar caps are formed by the condensation of atmospheric CO_2 during the polar night. Simple energy balance models can simulate this scenario quite well and accurately predict the general form of cap evolution and the surface pressure variation caused by this seasonal deposition of CO_2 frost.

However, we still do not understand many of the physical processes which control the seasonal caps, especially the residual south polar cap. Many details described in this chapter remain speculative:

1. We do not know what is really going on in the polar night during the cap formation: our most realistic scenario suggests that the reduced

infrared emission detected by Viking and Mariner 9, which is thought to reduce the condensation rate, is caused by CO_2 clouds and snow fall, but more evidence is needed.

2. Both observations and models suggest that dust and water ice should strongly affect the condensation and the sublimation phase of the caps through their impact on the radiative properties of both the atmosphere and the cap surface, on the atmospheric circulation, and on the formation of CO_2 clouds and snow. Within this context, the similarity of the pressure curves between years with and without dust storms is puzzling.

3. Which processes control the spatial and temporal variations of the albedo and the inhomogeneities throughout the spring and summer polar caps? Why do these processes create a north-south asymmetry?

4. The problems regarding the nature and the behavior of the residual CO_2 south polar cap are particularly subject to speculation. Why is it offset from the pole? Is the CO_2 ice residual cap a thick reservoir which can buffer the atmosphere or a thin cover which disappeared completely in 1969?

Fortunately, many of these questions will be addressed by future spacecraft missions. In particular, accurate measurements of the Martian topography, high spatial and temporal resolution infrared observations, gamma ray and neutron spectrometers will soon expand our knowledge of the polar caps and their control of the climate. However, these observations will likely raise many new questions and puzzles.

References

Air-liquide (1976). Encyclopédie des gaz. Elsevier publication.

Bell, J. F., and D. Crisp (1993), Groundbased imaging spectroscopy of Mars in the near infrared : preliminary results, *Icarus*, **104**, 2–19

Briggs, G. A., and C. B. Leovy (1974), Mariner 9 observations of the Mars north polar hood, *Bull. Am. Meteorol. Soc.*, **55**, 278–296

Briggs, G., K. Klaasen, T. Thorpe, and J. Wellman (1977) Martian dynamical phenomenon during June-November 1976: Viking orbiter imaging results, *J. Geophys. Res.*, **82**, 4121–4149

Briggs, G. A. (1974) The nature of the residual Martian polar caps, *Icarus*, **23**, 167–191

Butler, B., D. Muhleman, and M. Slade (1995), The difference in the residual ice caps on Mars as deduced from VLA/Goldstone radar images, Abstract for the "Solar System Ice" international symposium, Toulouse, France.

Calvin, W. M., and T. Z. Martin (1994) Spatial variability in the seasonal south polar cap of Mars, *J. Geophys. Res.*, **99**, 21,143–21,152

Calvin, W. M. (1990) Additions and corrections to the absorption coefficient of CO_2 ice : applications to the Martian south polar cap, *J. Geophys. Res.*, **95**, 14,743–14,750

Capen, C. F., and V. W. Capen (1970), Martian north polar cap (1962-1968, *Icarus*, **13**, 100–108.

Christensen, P. R., and R. W. Zurek (1984) Martian north polar hazes and surface ice: Results from the Viking survey/completion mission, *J. Geophys. Res.*, **89**, 4587–4596.

Clark, R. N., and T. B. McCord (1982) Mars residual polar cap : Earth-based spectroscopic confirmation of water ice as a major constituent and evidence for hydrated minerals, *J. Geophys. Res.*, **87**, 367–370

Colburn, D. S., J. B. Pollack, and R. M. Haberle (1989) Diurnal variations in optical depth at Mars, *Icarus*, **79**, 159–189

Davies, D. W., C. B. Farmer, and D. D. LaPorte (1979) Behavior of volatile in Mars' polar areas : a model incorporating new experimental data., *J. Geophys. Res.*, **82**, 3815–3822

Davies, D. W. (1979) Effect of dust on the heating of mars's surface and atmosphere, *J. Geophys. Res.*, **84**, 8289–8293

Ditteon, R., and H. H. Kieffer (1979) Optical properties of solid CO_2: Application to Mars, *J. Geophys. Res.*, **84**, 8294–8300

Dollfus, A. (1965) Etude de la planète Mars de 1954 à 1958, *Ann. Astrophys*, **28**, 722–747

Eluszkiewicz, J. (1993) On the microphysical state of the Martian seasonal caps, *Icarus*, **103**, 43–48

Fanale, F. P., Salvail, J., Banerdt, W. B., and Saunders, R. S. (1982). Mars: the regolith-atmosphere -cap system and climate change. *Icarus*, 50:381–407.

Forget, F., and J. Pollack (1996) Thermal infrared observations of the condensing Martian polar caps: CO_2 ice temperatures and radiative budget.,*J. Geophys. Res.*, **101**, 16,865–16,880

Forget, F., J. B. Pollack, and G. B. Hansen (1995) Low brightness temperatures of Martian polar caps : CO_2 clouds or low spectral emissivity?, *J. Geophys. Res.*, **100**, 21,119–21,234

Gierasch, P. J., and R. M. Goody (1968) A study of the thermal and dynamical structure of the Martian lower atmosphere, *Planet. Space Sci.*, **16**, 615–646

Haberle, R. M. (1995) Buried dry ice on mars, *Nature*, **374**, 595–596

Hansen, G. B. (1992) The spectral absorption of CO_2 ice from 0.18 to 4.8 microns, *Bull. Am. Astron. Soc.*, **24**, pp978

Hansen, G. B. (1993) The spectral absorption of CO2 ice in the thermal infrared, *Bull. Am. Astron. Soc.*, **25**, (3), 1034

Hart, H. M., and B. M. Jakosky (1986) Composition and stability of the condensate observed at the Viking lander 2 site on Mars, *Icarus*, **66**, 134–142

Herr, K. C., and G. C. Pimentel (1969) Infrared absorptions near three microns recorded over the polar caps of Mars, *Science*, **166**, 496–499

Herr, K. C., and G. C. Pimentel (1970) Evidence for solid carbon dioxide in the upper atmosphere of Mars, *Science*, **166**, 496–499

Herschel, W. (1784) On the remarkable appearance of the polar regions of the planet Mars, the inclination of its axis, the position of its poles, and its spheroidical figure; With a few hints relative to its diameter, *Philos. Trans.*, **24**, 233–273

Hess, S. L. (1979) Static stability and thermal wind in an atmosphere of variable composition: Application to Mars, *J. Geophys. Res.*, **84**, 2969–2973

Hourdin, F., P. Le Van, F. Forget, and O. Talagrand (1993) Meteorological variability and the annual surface pressure cycle on Mars, *J. Atmos. Sci.*, **50**, 3625–3640

Hourdin, F., F. Forget, and O. Talagrand (1995) The sensitivity of the Martian surface pressure to various parameters: a comparison between numerical simulations and Viking observations, *J. Geophys. Res.*, **100**, 5501–5523

Hunt, G. E. (1980) On the infrared radiative properties of CO2 ice clouds: Applications to Mars., *Geophys. Res. Lett.*, **7**, 481–484

Iwisaki, K., Y. Saito, and T. Akabane (1982) Martian north polar cap : 1979-1980, *J. Geophys. Res.*, **87**, 10265–10269

Jakosky, B. M., and E. S. Barker (1984) Comparison of ground-based and Viking Orbiter measurements of Martian water vapor : variability of the seasonal cycle., *Icarus*, **57**, 322–334

Jakosky, B. M., and R. M. Haberle (1990) Year-to-year instability of the Mars south polar cap., *J. Geophys. Res.*, **95**, 1359–1365

Jakosky, B. M., and T. Z. Martin (1987) Mars: North-polar atmospheric warming during dust storms, *Icarus*, **72**, 528–534

Jakosky, B. M., B. G. Henderson, and M. M. T. (1993) The Mars water cycle at other

epochs : recent history of the polar caps and layered terrain., *Icarus*, **102**, 286–297
Jakosky, B. M., B. G. Henderson, and M. T. Mellon (1995) Chaotic obliquity and the nature of the Martian climate, *J. Geophys. Res.*, **100**, 1579–1584
Jakosky, B. M. (1983) Comments on "Mars residual north polar cap : Earth-based spectroscopic confirmation of water ice as a major constituent and evidence for hydrated minerals" by R. N. Clark and T. B. McCord., *J. Geophys. Res.*, **88**, 4329–4330
James, P. B., and G. R. North (1982) The seasonal CO_2 cycle on Mars : An application of an energy balance climate model, *J. Geophys. Res.*, **87**, 10271–10283
James, P. B., G. Briggs, J. Barnes, and A. Spruck (1979) Seasonal recession of Mars' south polar cap as seen by Viking, *J. Geophys. Res.*, **84**, (B6), 2889–2922
James, P. B., M. Pierce, and L. J. Martin (1987) Martian north polar cap and circumpolar clouds: 1975-1980 Telescopic observation., *Icarus*, **71**, 306–312
James, P. B., H. H. Kieffer, and D. A. Paige (1992) The seasonal cycle of carbon dioxide on Mars, in *Mars*, pp. 934–968, University of Arizona Press, Tucson
James, P. B., R. T. Clancy, S. W. Lee, L. J. Martin, R. B. Singer, S. E., R. A. Kahn, and R. W. Zurek (1994) Monitoring Mars with the Hubble space telescope : 1990-1991 observations., *Icarus*, **109**, 79–101
James, P. B. (1979) Recession of Martian north polar cap : 1977-1978 Viking observations, *J. Geophys. Res.*, **84**, 8332–8334
James, P. B. (1982) Recession of Martian north polar cap : 1979-1980 Viking observations, *Icarus*, **52**, 565–569
James, P. B. (1983) Condensation phase of the Martian south polar cap, *Bull. Am. Astron. Soc.*, **15**, 846–847
Jones, K., R. E. Arvidson, E. A. Guiness, S. L. Braggs, S. D. Wall, C. E. Carlston, and D. G. Pidek (1979) One Mars year : Viking lander imaging observations, *Science*, **204**, 799–806
Kieffer, H. H., and A. P. Zent (1992) Quasi-periodic climate change on Mars, in *Mars*, edited by S. Kieffer, Jakosky and Matthews, pp. 1180–1218, University of Arizona Press, Tucson
Kieffer, H. H., S. C. Chase, E. D. Miner, F. D. Palluconi, G. Münch, G. Neugebauer, and T. Z. Martin (1976) Infrared thermal mapping of the martian surface and atmosphere: First results, *Science*, **193**, 780–786
Kieffer, H. H., T. Z. Martin, R. Peterfreund, B. M. Jakosky, E. D. Miner, and F. D. Palluconi (1977) Thermal and albedo mapping during the Viking primary mission, *J. Geophys. Res.*, **82**, 4249–4291
Kieffer, H. H. (1970*a*), Interpretation of the Martian polar cap spectra, *J. Geophys. Res.*, **75**, 510–514
Kieffer, H. H. (1970*b*), Spectral reflectance of CO_2-H_2O frosts, *J. Geophys. Res.*, **75**, 501–509
Kieffer, H. H. (1979) Mars south polar spring and summer temperatures: a residual co_2 frost, *J. Geophys. Res.*, **84**, 8263–8288
Larson, H. P., and U. Fink (1972) Identification of carbon dioxide frost on the Martian polar caps, *Astrophys. Jour.*, **171**, L91–L95
Laskar, J., and P. Robutel (1993) The chaotic obliquity of the planets, *Nature*, **361**, 608–612
Leighton, R. R., and B. C. Murray (1966) Behavior of carbon dioxide and other volatiles on Mars, *Science*, **153**, 136–144
Lindner, B. L. (1990) The Martian polar cap : radiative effects of ozone, clouds and airborne dust, *J. Geophys. Res.*, **95**, 1367–1379
Lindner, B. L. (1993) The hemispherical asymmetry in the Martian polar caps., *J. Geophys. Res.*, **98**, 3339–3344
Lumme, K., and P. B. James (1984) Some photometric properties of the Martian south polar cap region during the 1971 apparition., *Icarus*, **58**, 363–376
Lumme, K. (1976) On the surface brightness and geometric albedo of some Martian areas., *Icarus*, **29**, pp69

Martin, T. Z., and H. H. Kieffer (1979) Thermal infrared properties of the Martian atmosphere, 2, the 15μm band measurements, *J. Geophys. Res.*, **84**, 2843–2852
Martin, T. Z. (1981) Mean thermal and albedo behavior of the Mars surface and atmosphere over a Martian year, *Icarus*, **45**, 427–446
Ono, A., and D. A. Paige (1995) Martian polar frosts, Abstract for the "Solar System Ice" international symposium, Toulouse, France
Paige, D. A., and A. P. Ingersoll (1985) Annual heat balance of Martian polar caps: Viking observations, *Science*, **228**, 1160–1168
Paige, D. A., and S. E. Wood (1992) Modeling the Martian seasonal CO_2 cycle: 2. interannual variability, *Icarus*, **99**, 15–27
Paige, D. A., D. Crisp, and M. L. Santee (1990*a*), It snows on mars, *Bull. Am. Astron. Soc.*, **22**, 1075
Paige, D. A., K. E. Herkenhoff, and B. C. Murray (1990*b*), Mariner 9 observations of the south polar cap of Mars : evidence for residual CO_2 frost, *J. Geophys. Res.*, **95**, 1319–1335
Paige, D. A. (1985) The annual heat balance of the Martian polar caps from Viking observations, Ph.D. thesis, Calif. Inst. of Technol., Pasadena
Parker, D. C., C. F. Capen, and J. D. Beish (1983) Exploring the martian artic., *Sky & Telescope*, **65**, 218–220
Pimentel, G., P. Forney, and K. Herr (1974) Evidence about hydrate and solid water in the Martian surface from the 1969 Mariner infrared spectrometer, *J. Geophys. Res.*, **79**, 1623–1634
Pollack, J. B., R. M. Haberle, J. Schaeffer, and H. Lee (1990) Simulations of the general circulation of the Martian atmosphere, I, Polar processes, *J. Geophys. Res.*, **95**, 1447–1473
Pollack, J. B., R. M. Haberle, J. R. Murphy, J. Shaeffer, and H. Lee (1993) Simulation of the general circulation of the Martian atmosphere II: seasonnal pressure variations, *J. Geophys. Res.*, **98**, (E2), 3149–3181
Rizk, B., R. M. Haberle, D. Hunten, and J. B. Pollack (1995) Meridional transport and water reservoir in southern Mars during 1988-1989, *Icarus*, **118**, 39–50
Svitek, T., and B. Murray (1990) Winter frost at Viking Lander 2 site, *J. Geophys. Res.*, 1495–1510
Talagrand, O., F. Hourdin, and F. Forget (1991) The LMD Martian general circulation model: Results about the annual pressure cycle, *Bull. Am. Astron. Soc.*, **23**, 1217 (oral presentation at the 23rd annual DPS meeting (Palo Alto, California).
Tillman, J. E., and W. Guest (1987) a, technical report, National Space Sciences Data Center
Tillman, J. E. (1988) Mars global atmospheric oscillations: Annually synchronized transient normal-mode oscillations and the triggering of global dust storms, *J. Geophys. Res.*, **93**, 9433–9451
Wall, S. D. (1981) Analysis of condensates formed at the Viking 2 lander site : the first winter, *Icarus*, **47**, 173–183
Ward, W. R., B. C. Murray, and M. C. Malin (1974) Climatic variations on Mars. 2. Evolution of carbon dioxide atmosphere and polar caps, *J. Geophys. Res.*, **79**, 3387–3395
Warren, S. G., W. J. Wiscombe, and J. F. Firestone (1990) Spectral albedo and emissivity of CO_2 in Martian polar caps: model results, *J. Geophys. Res.*, **95**, 717–741
Warren, S. G. (1986) Optical constants of carbon dioxide ice, *Appl. Opt.*, **25**, 2650–2674
Washburn, E. (1948). *International critical tables of numerical data,physics, chemistry, and technology, volume 3.* New York: McGraw Hill.
Wood, S. E., and D. A. Paige (1992) Modeling the martian seasonal CO_2 cycle: fitting the Viking lander pressure curves, *Icarus*, **99**, 1–14
Zurek, R. W., and L. J. Martin (1993) Interannual variability of planet-encircling dust storms on Mars, *J. Geophys. Res.*, *98*, 3247–3259